Supplementary Information (SI)

Structure and Energetics of Low-index Stoichiometric $BiPO_4$ Surfaces

Yuan Xu,[a] Xinguo Ma,*,[a] Jisong Hu,[a] Ang Xu,[b] Zhuoran Wang,[c] Chuyun Huang*,[a]

[a] *School of Science and Hubei Collaborative Innovation Center for High-efficiency Utilization of Solar Energy, Hubei University of Technology, Wuhan 430068, China;*

[b] *State Grid Wuhan Dongxihu District Electric Power Supply Company, Wuhan 430040, China.*

[c] *School of Optical and Electronic Information, Huazhong University of Science and Technology, Wuhan 430074, China.*

E-mail: maxg2013@sohu.com (X.G. Ma); chuyunh@163.com (C.Y. Huang)

1. Corrected surface energy

Here, we proposed a new scheme to correct the average surface energies and to obtain a more precise result by the relation of the surface energies between fixed two lateral faces and fixed one lateral faces. The relation can be expressed as

$$E_{\mathrm{surf/(rel-top)}} + E_{\mathrm{surf/(fix-bot)}} = 2E_{\mathrm{surf/(fix-1Face)}} \quad \text{(S1)}$$

$$E_{\mathrm{surf/(fix-top)}} + E_{\mathrm{surf/(fix-bot)}} = 2E_{\mathrm{surf/(fix-2Face)}} \quad \text{(S2)}$$

$$E_{\mathrm{surf/(fix-top)}} = E_{\mathrm{surf/(fix-bot)}} \quad \text{(S3)}$$

where $E_{\mathrm{surf/(rel-top)}}$ and $E_{\mathrm{surf/(fix-bot)}}$ represent the surface energies for the relaxed top lateral face and the unrelaxed bottom lateral face, respectively, when only the top lateral face is permitted to optimize in the formula S1. For the formula S2, $E_{\mathrm{surf/(fix-top)}}$ and $E_{\mathrm{surf/(fix-bot)}}$ are the surface energies for the top lateral face and the bottom lateral face, respectively, when both of two lateral faces are fixed. It is easy to understand that $E_{\mathrm{surf/(fix-top)}}$ is equal to $E_{\mathrm{surf/(fix-bot)}}$, due to their same situations when two lateral faces are fixed, namely, the same surface dangling bond and the fixation of two lateral faces. Lastly, according to formula S1, S2, and S3, the corrected surface energy for the relaxed top lateral face can be obtained as follow:

$$E_{\mathrm{surf/(rel-top)}} = 2E_{\mathrm{surf/(fix\text{-}1Face)}} - E_{\mathrm{surf/(fix\text{-}2Face)}} \quad \text{(S4)}$$

Of course, the $E_{\mathrm{surf/(fix-1Face)}}$ and $E_{\mathrm{surf/(fix-2Face)}}$ can be gained by the average surface energy $E_{\mathrm{surf}} = (E_{\mathrm{slab}} - \mathrm{N}E_{\mathrm{bulk}})/2S$.

2. Crystal structure of bulk $BiPO_4$

Table S1. Lattice constants of monazite $BiPO_4$. Ref. 10 and 40 are for the experimental data.

a(Å)	b(Å)	c(Å)	β(°)	
6.763	6.952	6.482	103.74	Ref. 10
6.752	6.912	6.470	103.64	Ref. 40
6.845	7.083	6.487	104.26	This work

Table S2. Ball and stick structures of two PO_4 tetrahedrons and BiO_n polyhedra.

Polyhedra	Structure
BiO_6	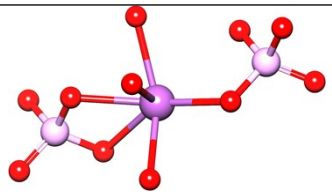
BiO_7	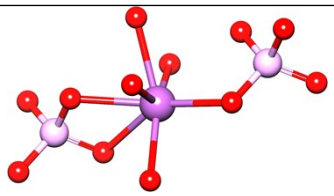
BiO_8	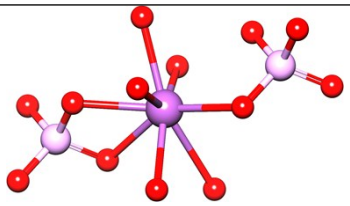
BiO_9	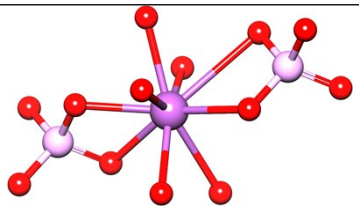

In Fig. 1, four type of oxygen atoms exist in the PO_4 tetrahedron, which are marked by ‘‘a’’ to ‘‘d’’. Likewise, subscripts from “A” to “I”, indicate the type of oxygen atoms in BiO_9 polyhedra. The PO_4 and BiO_n are combined into a chain structure along c-axis which are pick up from the supercells of the bulk structure of $BiPO_4$. Two edges of one BiO_9 polyhedra shares four O atoms with two adjacent PO_4 units to form a linear chain of alternate PO_4 and BiO_9 units, while one BiO_n (where n=6, 7, 8) polyhedra shares three O atoms with two adjacent PO_4 units to make a linear chain [1–4].

Reference

[1] S.N. Achary, D. Errandonea, A. Muñoz, Experimental and theoretical investigations on the polymorphism and metastability of $BiPO_4$, Dalton Trans. 42 (2013) 14999–15015.

[2] R.C.L. Mooney-Slater, Polymorphic forms of bismuth phosphate. Zeitschrift für Kristallographie-Crystalline Materials. 117 (1962) 371–385.

[3] C.S. Pan, Y.F. Zhu, A review of $BiPO_4$, a highly efficient oxyacid-type photocatalyst, used for environmental applications, Catal. Sci. Technol. 5 (2015) 3071–3083.

[4] L. Zhu, X.G. Ma, Y. Wei, L. Chu, H. H. Wang, C.Y. Huang, Origin of photocatalytic activity of $BiPO_4$: the first-principles calculations, Chinese J. Struc. Chem. 8 (2017) 1299–1306.

Table S3. Bond lengths and bond angles of monazite $BiPO_4$ in PO_4 tetrahedron and BiO_6 polyhedra.

Label	Bond length (Å)	Label	Bond angle (°)
$P–O_a$	1.526	$\angle O_a\text{-}P\text{-}O_b$	115.988
$P–O_b$	1.529	$\angle O_a\text{-}P\text{-}O_c$	113.917
$P–O_c$	1.543	$\angle O_b\text{-}P\text{-}O_c$	105.527
$P–O_d$	1.560	$\angle O_c\text{-}P\text{-}O_d$	110.502
$Bi–O_A$	2.353	$\angle O_A\text{-}Bi\text{-}O_B$	70.214
$Bi–O_B$	2.382	$\angle O_B\text{-}Bi\text{-}O_C$	85.252
$Bi–O_C$	2.397	$\angle O_C\text{-}Bi\text{-}O_D$	81.564
$Bi–O_D$	2.417	$\angle O_D\text{-}Bi\text{-}O_E$	99.526
$Bi–O_E$	2.449	$\angle O_E\text{-}Bi\text{-}O_F$	112.375
$Bi–O_F$	2.555	$\angle O_A\text{-}Bi\text{-}O_F$	121.891

Table S4. Bond lengths of monazite $BiPO_4$ in PO_4 tetrahedron and BiO_9 polyhedra. The lengths of P–O bonds are mostly around 1.5 Å without apparent fluctuation. In contrast, the bond length of Bi–O has a range from 2.35 Å to 3.02 Å. The longer the bond length, the less force between atoms, which results in the weak mutual influence between atoms.

PO_4	Bond length (Å)	BiO_9	Bond length (Å)
$P–O_a$	1.526	$Bi–O_A$	2.353
$P–O_b$	1.529	$Bi–O_B$	2.382
$P–O_c$	1.543	$Bi–O_C$	2.397
$P–O_d$	1.560	$Bi–O_D$	2.417
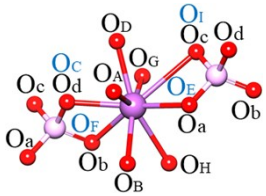		$Bi–O_E$	2.449
		$Bi–O_F$	2.555
		$Bi–O_G$	2.653
		$Bi–O_H$	2.750
		$Bi–O_I$	3.020

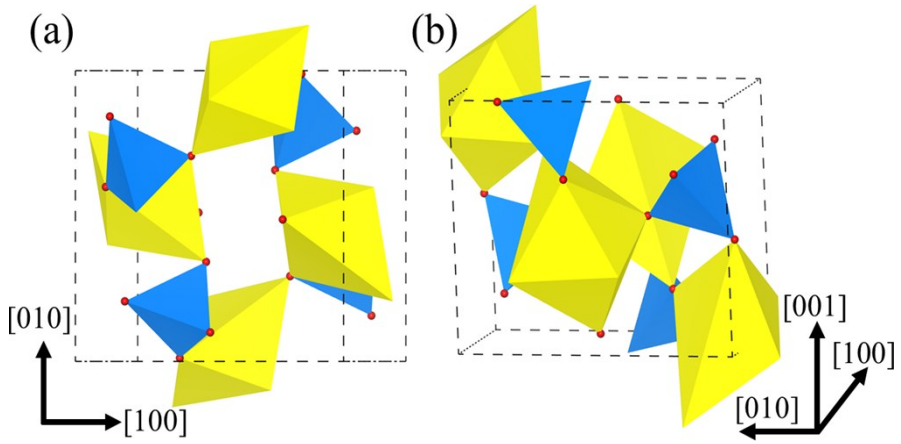

Fig. S1. Polyhedral model of monoclinic monazite $BiPO_4$ along (a) [001] direction and (b) [100] direction. The yellow octahedron and blue tetrahedra represent BiO_6 and PO_4, respectively.

Table S5. Supercell structures of monazite $BiPO_4$ along x-, y- and z-axis, respectively. Bi and P atoms are alternately arranged along the z-axis while P and Bi atoms form two single main chains along x-axis and y-axis, which exhibit the characteristics of a layered structure for monazite $BiPO_4$.

Supercell	Side view	Top view
4×1×1	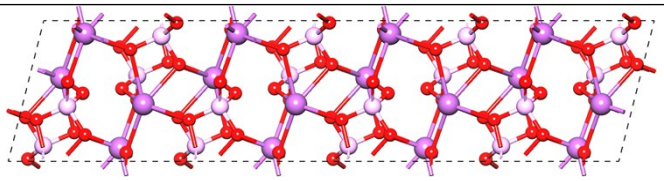	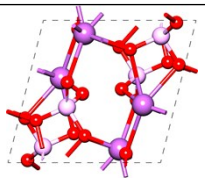
1×4×1	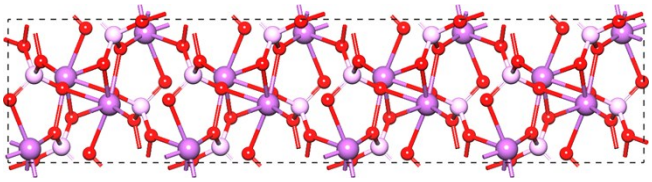	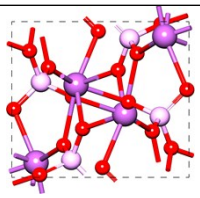
1×1×4	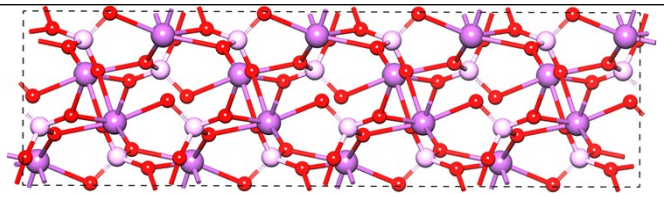	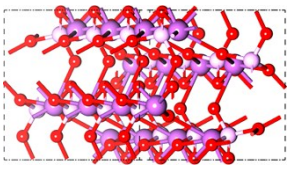

3. All possible termination surfaces

Table S6. Total energies and their convergences of possible stoichiometric terminations of four surface structures.

Surface	Type	Slice	Structure	E_{slab} (eV)	Convergence (eV/atom)
001	A	0.063	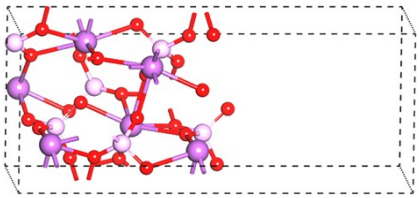	-12480.958	3.010×10^{-4}
	B	0.169	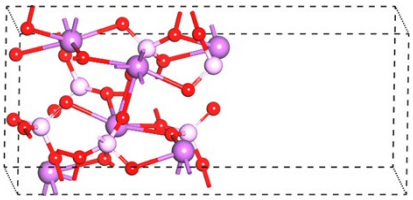	-12482.250	7.759×10^{-6}
	C	0.252	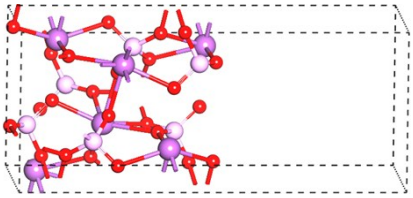	-12484.738	4.726×10^{-3}
	D	0.358	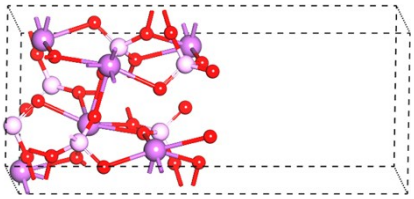	-12482.052	3.140×10^{-4}
	E	0.487	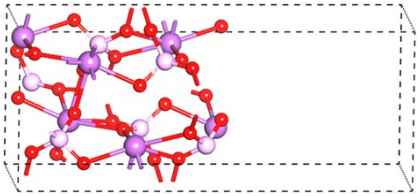	-12483.870	4.013×10^{-2}
010	A	0.252	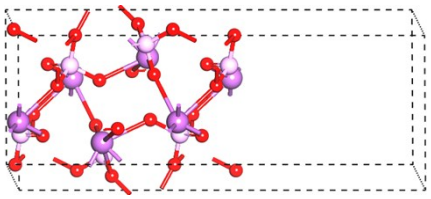	-12484.680	2.269×10^{-2}
	B	0.325	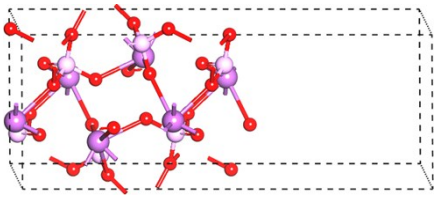	-12480.817	3.751×10^{-2}

	C	0.492	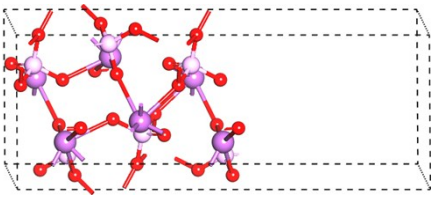	-12490.205	7.294×10^{-5}
011	A	0.390	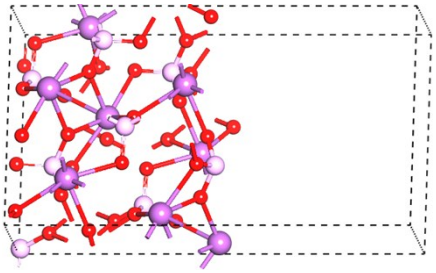	-16605.130	-7.216×10^{-6}
	B	0.957	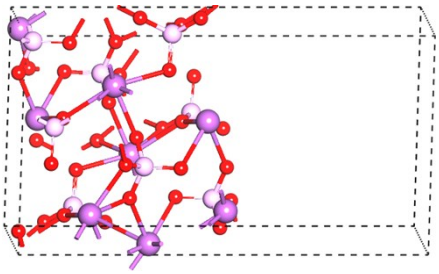	-16620.611	1.485×10^{-4}
100	A	0.084	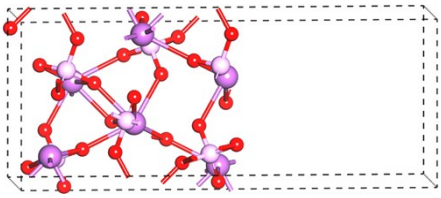	-12487.316	2.452×10^{-6}
	B	0.204	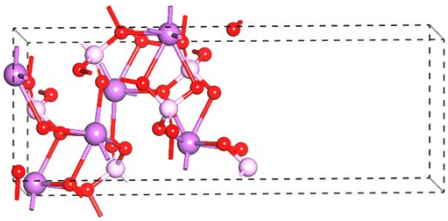	-12481.703	4.600×10^{-5}
	C	0.459	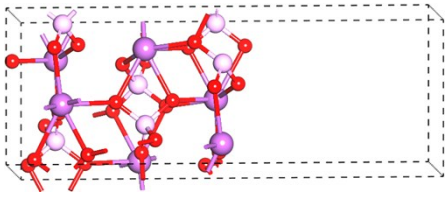	-12487.339	7.517×10^{-6}
	D	0.500	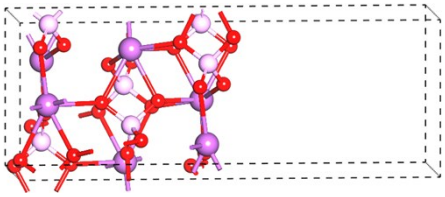	-12489.852	1.065×10^{-5}

4. Incomplete PO_4 tetrahedron along (001) plane

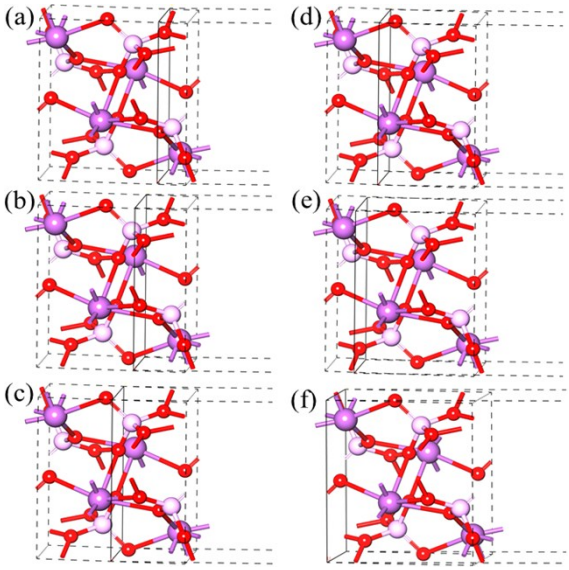

Fig. S2. All possible slices with incomplete PO_4 tetrahedrons along the (001) plane. Here, panels (a)-(f) show the six possible slices at the points 0.2, 0.35, 0.5, 0.65, 0.8, 1.0 along (001) plane, respectively. It can be found that keeping intact PO_4 tetrahedrons in the stoichiometric (001) surface is impossible.

5. Surface structure parameters

Table S7. The structure parameters of the (001) surface before and after relaxation. Atom labels refer to Fig. 1(c) and Fig. 2(b).

	Unrelaxed			**Relaxed**			
Atom	**X_1**	**Y_1**	**Z_1**	**X_2**	**Y_2**	**Z_2**	**d/ Å**
$O_{(1)}$	0.800	2.845	8.745	0.915	2.953	8.742	0.158
$O_{(2)}$	1.284	5.605	8.853	1.375	5.811	9.241	0.448
Bi	6.051	4.509	8.155	6.170	4.272	8.167	0.265
P	2.661	5.903	8.260	2.420	5.83	8.226	0.254
Bond	**Length/ Å**			**Length/ Å**		**Δ/ Å**	**Ratio (%)**
Bi–O	2.382			2.255		-	-5.33
P–O_a	1.526			1.491		-	-2.29
P–O_b	1.529			1.457		-	-4.71
P–O_c	1.543			1.485		-	-3.76
Angle	**/°**			**/°**		**Δ/ °**	**Ratio (%)**
∠O_a-P-O_c	106.89			114.65		7.76	7.26
∠O_b-P-O_c	113.08			123.70		10.62	9.39

∠O_a-P-O_b	115.09	121.64	6.55	5.69

Table S8. The structure parameters of the (010) surface before and after relaxation. Atom labels refer to Fig. 1(c) and Fig. 3(b).

	Unrelaxed			Relaxed			
Atom	**X_1**	**Y_1**	**Z_1**	**X_2**	**Y_2**	**Z_2**	**d/ Å**
$O_{(1)}$	4.437	2.181	10.365	4.118	2.181	10.180	0.369
$O_{(2)}$	0.389	3.547	9.746	0.170	3.514	9.798	0.228
Bi	2.214	2.398	9.486	1.896	2.315	9.280	0.388
P	5.558	2.437	9.295	5.378	2.438	9.298	0.180
Bond	**Length/ Å**			**Length/ Å**		**Δ/ Å**	**Ratio (%)**
Bi–O	2.397			2.388		-0.009	-0.38
P–O_a	1.526			1.507		-0.019	-1.25
P–O_b	1.529			1.575		0.046	3.01
P–O_c	1.543			1.573		0.030	1.94
Angle	**/°**			**/°**		**Δ/ °**	**Ratio (%)**
∠O_a-P-O_c	106.89			107.10		0.21	0.196
∠O_b-P-O_c	113.08			110.20		-2.88	-2.55
∠O_a-P-O_b	115.09			114.45		-0.64	-0.56

Table S9. The structure parameters of the (011) surface before and after relaxation. Atom labels refer to Fig. 1(c) and Fig. 4(b).

	Unrelaxed			Relaxed			
Atom	**X_1**	**Y_1**	**Z_1**	**X_2**	**Y_2**	**Z_2**	**d/ Å**
$O_{(1)}$	4.368	6.333	8.746	4.546	6.493	8.766	0.240
$O_{(2)}$	6.706	5.312	8.746	6.917	5.141	8.820	0.282
Bi	2.214	2.398	9.486	1.896	2.315	9.280	0.388
P	5.558	2.437	9.295	5.378	2.438	9.298	0.180
Bond	**Length/ Å**			**Length/ Å**		**Δ/ Å**	**Ratio (%)**
Bi–O	2.397			2.254		-	-5.97
P–O_a	1.526			1.560		0.034	2.23
P–O_b	1.529			1.536		0.007	0.46
P–O_c	1.543			1.531		-	-0.78

Angle	/°	/°	Δ/ °	Ratio (%)
∠O_a-P-O_c	106.89	107.35	0.45	0.42
∠O_b-P-O_c	113.08	114.55	1.47	1.30
∠O_a-P-O_b	115.09	109.30	-5.79	-5.03

Table S10. The structure parameters of the (100) surface before and after relaxation. Atom labels refer to Fig. 1(c) and Fig. 5(b).

	Unrelaxed			Relaxed			
Atom	**X_1**	**Y_1**	**Z_1**	**X_2**	**Y_2**	**Z_2**	**d/ Å**
$O_{(1)}$	0.701	5.325	9.362	0.880	5.451	9.377	0.219
$O_{(2)}$	4.962	5.340	8.867	4.855	5.303	8.888	0.115
Bi	0.963	0.957	8.247	1.035	0.779	8.023	0.295
P	1.154	4.292	8.285	1.191	4.320	8.376	0.102
Bond	**Length/ Å**			**Length/ Å**		**Δ/ Å**	**Ratio (%)**
Bi–O	2.353			2.399		0.046	1.96
P–O_a	1.526			1.525		-0.001	-0.067
P–O_b	1.529			1.605		0.076	4.97
P–O_c	1.543			1.526		-0.017	-1.10
Angle	**/°**			**/°**		**Δ/ °**	**Ratio (%)**
∠O_a-P-O_c	106.89			107.46		0.57	0.53
∠O_b-P-O_c	113.08			110.22		-2.86	-2.53
∠O_a-P-O_b	115.09			111.495		-3.60	-3.12

6. Planar averaged charge density difference

To specifically illustrate the effect of surface relaxation, the planar-averaged electron density difference of the surface before and after relaxation is calculated along the z direction. It is defined as

$$\Delta\rho(z) = \int \rho_{\text{relaxed}}(x,y,z)dxdy - \int \rho_{\text{unrelaxed}}(x,y,z)dxdy \quad \text{(S5)}$$

where $\rho_{\text{relaxed}}(x,y,z)$ and $\rho_{\text{unrelaxed}}(x,y,z)$ are the charge density of relaxed and unrelaxed surfaces at the (x, y, z) point, respectively. The positive values indicate electrons accumulation, while the negative values represent the depletion of electrons.

7. Intact PO_4 tetrahedron in the (100) surface

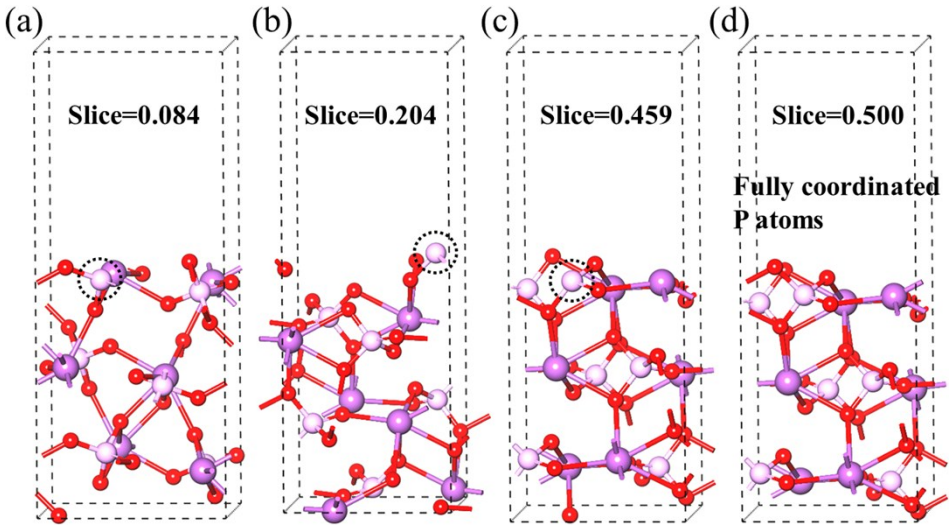

Fig. S3. All possible terminations along the (100) plane. Here, panels (a)-(d) show the four possible slices at the points 0.084, 0.204, 0.459 and 0.500, respectively. And only picture (d) with top 0.500 shows the intact PO_4 tetrahedron.

Table S11. The atomic displacements from the bulk-truncated ideal positions, and the expansion ratios of bond length and bond angle in the outermost layer after the relaxation of (100) surface. Here, the two slices are considered at the points 0.459 and 0.500. The corresponding atom labels are shown in Fig. 1(c) and Fig. 5(b). Among three possible terminations (see Fig. S3(a), S3(b) and S3(c) with incomplete PO_4 tetrahedrons in (100) surface, the termination in Fig. S3(c) is the most stable, so it is set as reference to compare with that in Fig. S3(d).

Slice	Atom	Δx /Å	Δy /Å	Δz /Å	d /Å	Bond	Ratio /%	Angle	Ratio /%
0.459	$O_{(1)}$	0.02	-0.05	0.03	0.06	Bi-O	-3.86	$\angle O_a$-P-O_c	0.93
	$O_{(2)}$	0.10	0.06	-0.06	0.13	P-O_a	1.44	$\angle O_b$-P-O_c	-1.95
	Bi	0.04	-0.19	-0.27	0.33	P-O_b	4.71	$\angle O_a$-P-O_b	-3.72
	P	0.03	0.003	0.1	0.10	P-O_c	-0.97	—	
0.500	$O_{(1)}$	0.18	0.22	0.02	0.22	Bi–O	1.96	$\angle O_a$-P-O_c	0.53
	$O_{(2)}$	-0.11	-0.04	0.02	0.12	P–O_a	-0.07	$\angle O_b$-P-O_c	-2.53
	Bi	0.07	-0.16	-0.22	0.30	P–O_b	4.97	$\angle O_a$-P-O_b	-3.12
	P	0.04	0.03	0.09	0.10	P–O_c	-1.10	—	

8. Proportion of crystal shape area

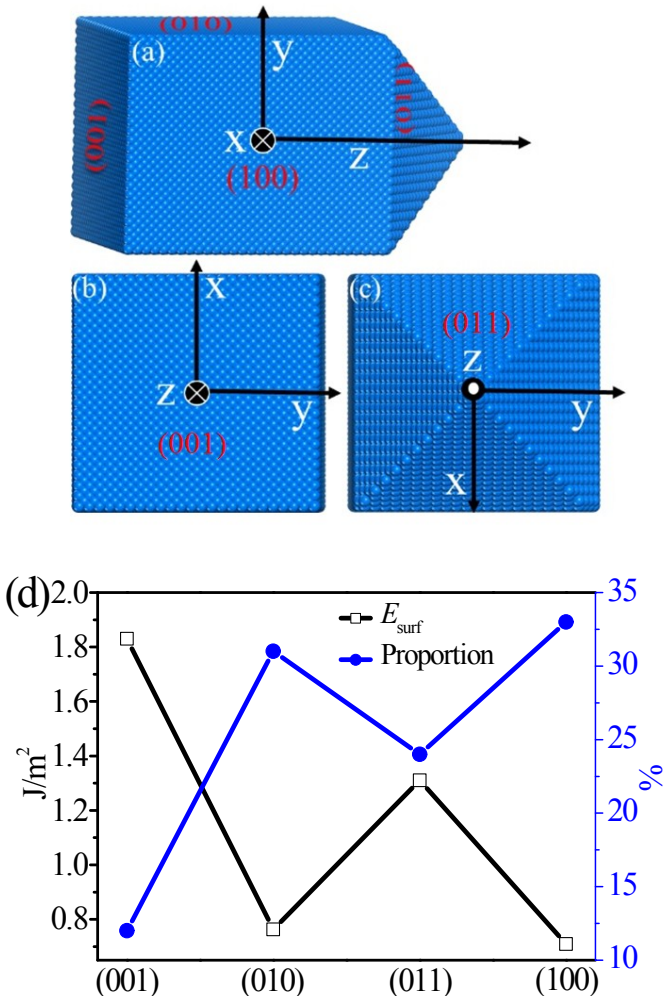

Fig. S4. Perspective view (a), bottom view (b), top view (c) of the equilibrium shape of $BiPO_4$ crystal in the monoclinic monazite phase, according to the Wulff construction and the average surface energies. (d) The relation between the average surface energies and the proportions of crystal shape area.